A small-molecule inhibitor of TRPC5 ion channels suppresses progressive kidney disease in animal models

Citation: Zhou, Yiming et al. "A Small-Molecule Inhibitor of TRPC5 Ion Channels Suppresses Progressive Kidney Disease in Animal Models." Science 358, 6368 (December 2017): 1332–1336

As Published: http://dx.doi.org/10.1126/SCIENCE.AAL4178

Publisher: American Association for the Advancement of Science (AAAS)

Persistent URL: http://hdl.handle.net/1721.1/116684

Version: Author's final manuscript: final author's manuscript post peer review, without publisher's formatting or copy editing

HHS Public Access

Author manuscript

Science. Author manuscript; available in PMC 2018 June 22.

Published in final edited form as:

Science. 2017 December 08; 358(6368): 1332–1336. doi:10.1126/science.aal4178.

A small-molecule inhibitor of TRPC5 ion channels suppresses progressive kidney disease in animal models

Yiming Zhou[1,2,*], **Philip Castonguay**[1,2,*], **Eriene-Heidi Sidhom**[1,2], **Abbe R. Clark**[1,2], **Moran Dvela-Levitt**[1,2], **Sookyung Kim**[1,2], **Jonas Sieber**[1,2], **Nicolas Wieder**[1,2], **Ji Yong Jung**[1,3], **Svetlana Andreeva**[1], **Jana Reichardt**[1], **Frank Dubois**[1], **Sigrid C. Hoffmann**[4], **John M. Basgen**[5], **Mónica S. MontesinoS**[1,2], **Astrid Weins**[1,6], **Ashley C. Johnson**[7], **Eric S. Lander**[2], **Michael R. Garrett**[7], **Corey R. Hopkins**[8], and **Anna Greka**[1,2,†]

[1]Department of Medicine, Brigham and Women's Hospital and Harvard Medical School, Boston, MA 02115, USA

[2]Broad Institute of MIT and Harvard, Cambridge, MA 02142, USA

[3]Department of Internal Medicine, Gachon University Gil Medical Center, Incheon, Republic of Korea

[4]Medical Research Center, Medical Faculty Mannheim, University Heidelberg, Germany

[5]Life Sciences Institute, Charles R. Drew University of Science and Medicine, Los Angeles, CA 90059, USA

[6]Department of Pathology, Brigham and Women's Hospital, Boston, MA 02115, USA

[7]Department of Pharmacology and Toxicology, University of Mississippi Medical Center, Jackson, MS 39216, USA

[8]Department of Pharmaceutical Sciences, University of Nebraska Medical Center, Omaha, NE 68198, USA

Abstract

Progressive kidney diseases are often associated with scarring of the kidney's filtration unit, a condition called focal segmental glomerulosclerosis (FSGS). This scarring is due to loss of podocytes, cells critical for glomerular filtration, and leads to proteinuria and kidney failure. Inherited forms of FSGS are caused by Rac1-activating mutations, and Rac1 induces TRPC5 ion channel activity and cytoskeletal remodeling in podocytes. Whether TRPC5 activity mediates FSGS onset and progression is unknown. We identified a small molecule, AC1903, that specifically blocks TRPC5 channel activity in glomeruli of proteinuric rats. Chronic administration of AC1903 suppressed severe proteinuria and prevented podocyte loss in a

[†]Corresponding author. Email: agreka@bwh.harvard.edu.
[*]These authors contributed equally to this work.

SUPPLEMENTARY MATERIALS

www.sciencemag.org/content/358/6368/1332/suppl/DC1

Materials and Methods
Figs. S1 to S10
Tables S1 and S2
References (35, 36)

transgenic rat model of FSGS. AC1903 also provided therapeutic benefit in a rat model of hypertensive proteinuric kidney disease. These data indicate that TRPC5 activity drives disease and that TRPC5 inhibitors may be valuable for the treatment of progressive kidney diseases.

Progressive chronic kidney diseases affect more than 500 million people worldwide and are increasing in prevalence (1,2). As a leading cause of kidney failure, focal segmental glomerulosclerosis (FSGS) in its most severe form is associated with the nephrotic syndrome, which is diagnosed on the basis of proteinuria, the spilling of essential proteins into the urine, and histopathologic findings including scarring in large segments of the glomerulus, the filtering unit of the kidney (3). This scarring is due to injury and loss of terminally differentiated cells of the kidney filter, the podocytes (3,4). Both the proteinuria and the histopathologic abnormalities contribute to patient symptoms (such as severe edema and shortness of breath) and increase the risk of kidney failure, heart failure, and premature death (3). Current therapy for FSGS consists of off-label use of nonspecific medications, which do not alter the progression of disease and are associated with toxicities (3).

Inherited and sporadic forms of FSGS are caused by mutations in genes that encode regulators of the actin cytoskeleton (5)—specifically, modulators of Rac1. Mutations in these genes, including *ARHGAP24* (6), *ARHGDIA* (7), and *ARHGEF17* (8), result in excess Rac1 signaling in podocytes (6–8). Activation of Rac1 signaling leads to the vesicular insertion of transient receptor potential canonical-5 (TRPC5) ion channels into the podocyte plasma membrane, making them available for activation by receptors such as the angiotensin II type 1 receptor (AT1R) (9,10). This results in transient Ca^{2+} influx into the podocyte, and further Rac1 activation, feeding a circuit that promotes podocyte cytoskeletal remodeling (10–12). Because little is known about the pathophysiologic role of the Rac1-TRPC5 pathway in the onset and progression of FSGS, which is the result of podocyte loss (3), we investigated two critical questions: Is this pathway responsible for disease progression in FSGS and, if so, can it be blocked for therapeutic benefit?

To study the role of Rac1-TRPC5–mediated podocyte injury in FSGS, we used AT1R transgenic (TGNeph-hAT1R/185 or AT1R Tg) rats, which express the human AT1R in a podocyte-specific manner (13). Similar to FSGS patients (3), these rats develop all the classical features of nephrotic syndrome (13, 14). Because they have podocyte-specific expression of the AT1R, these animals do not experience any of the systemic effects of excess angiotensin signaling, such as hypertension or vascular disease (13), thus allowing us to focus on podocyte-specific pathology. In our studies, AT1R Tg rats developed severe, progressive proteinuria over the course of 50 weeks, with onset of disease at 8 to 14 weeks and severe escalation in proteinuria beyond 14 weeks (fig. S1A). As a consequence of their progressive kidney failure, AT1R Tg rats died at an average age of 400 days, whereas wild-type (WT) control rats lived beyond 700 days (fig. S1B). In these studies, we focused on AT1R Tg rats with established disease (Advanced, ~18 weeks), defined by severe proteinuria (>25 mg/day), and compared them to younger rats with early disease (Onset, ~12 weeks, >5 mg/day proteinuria) (fig. S1A).

We examined TRPC channel activity in isolated rat glomeruli by recording podocyte Ca^{2+} transients in response to angiotensin II (AngII). These experiments suggested that the

lanthanum (La^{3+})- sensitive TRPC6 plays a homeostatic role in WT glomeruli, but TRPC5, unmasked by La^{3+}, shows increased activity early on (Onset) and predominates during disease progression (Advanced) (fig. S2, A and B). To confirm these results, we used patch-clamp electrophysiology adapted to the isolated glomeruli preparation. We tested riluzole, a direct activator of TRPC5 channel activity (15), and ML204, a tool compound that blocks TRPC5 (16). In inside-out recordings of podocytes from AT1R Tg rat glomeruli isolated at disease onset, we recorded significant ML204 inhibition of channel activity. In glomeruli from rats with established disease (Advanced), riluzole activated a large TRPC5 conductance, which was blocked by ML204 (Fig. 1, A and B, and fig. S3, A and B). By contrast, we recorded minimal riluzole-mediated TRPC5 activation in WT rat glomeruli in age-matched controls (Fig. 1, A and B, and fig. S3, A and B). To examine effects on TRPC6 channels, we used 1-oleoyl-2-acetyl-glycerol (OAG), which directly activates these channels (17). We noted no inhibition of ML204 on OAG-induced conductances in recordings from age-matched AT1R Tg rats and WT controls (fig. S3C). We therefore excluded the possibility that the effect of ML204 can be explained by its targeting of TRPC6 channel activity in AT1R Tg rats at any stage of disease progression (fig. S3C). The conclusion from Ca^{2+} imaging and electrophysiology in rat glomeruli is that TRPC5-mediated Ca^{2+} influx in podocytes correlates with FSGS disease progression (Fig. 1C).

We next tested the efficacy of ML204 in vivo. Intraperitoneal administration of ML204 twice daily for 7 days to animals at disease onset induced remission of proteinuria: Urine protein concentrations in treated rats were comparable to those in WT controls (fig. S4, A and B). Furthermore, administration of ML204 (25 mg/kg) twice daily over the course of 14 days in rats with severe disease (Advanced) suppressed progression of proteinuric disease at 7 days and 14 days (Fig. 1D) without evidence of toxicity (fig. S4, C to G). Control AT1R Tg animals continued to have escalating proteinuria (Fig. 1D). Morphometric analysis (18,19) (see methods) showed that ML204 prevented podocyte loss in AT1R Tg rats with advanced disease, maintaining the numbers of podocytes at near-baseline WT levels, in contrast to significant podocyte loss in control phosphate-buffered saline (PBS)–treated AT1R Tg rats (Fig. 1E). AT1R Tg rats with advanced disease also had numerous podocyte pseudocysts (fig. S4H), similar to previously described pseudocysts leading to podocyte loss through detachment from the basement membrane in various models of FSGS (20). Treatment with ML204 prevented pseudocyst formation, suggesting that podocytes were rescued from detachment and loss (fig. S4, H and I). Thus, podocyte numbers are preserved by treatment with ML204.

Because ML204 blocks TRPC5 and TRPC4 channels, and weakly blocks TRPC6 channels (16), we set out to develop a more specific TRPC5 inhibitor. We sought a compound with podocyte-protective properties and no unwanted on-target effects on TRPC4 channels [which, although not expressed in podocytes (10), are expressed in endothelium (21)] or TRPC6 channels. Based on the structures of published blockers (16,22), we synthesized and tested a series of 50 molecules for activity against TRPC5, TRPC4, and TRPC6 and identified compound AC1903 (Fig. 2A) as a promising candidate. Patch-clamp electrophysiology experiments in human embryonic kidney 293 (HEK-293) cells expressing TRPC5, TRPC4, or TRPC6 revealed that AC1903 is TRPC5-selective: In dose-response experiments, it blocked riluzole-activated TRPC5 whole-cell current, but failed to block

carbachol (CCh)–induced TRPC4 and OAG-induced TRPC6 currents, even at high micromolar concentrations (Fig. 2B and fig. S5, A to C). We also compared the dose responses of AC1903 and ML204 and found that the two inhibitors were nearly equipotent, with half-maximal inhibitory concentration of ML204 ($IC_{50\ ML204}$) = 13.6 μM versus $IC_{50\ AC1903}$ = 14.7 μM (Fig. 2C). In standard kinase profiling assays, AC1903 did not have offtarget effects (table S1). Thus, AC1903 selectively blocks TRPC5 ion channels.

Rac1 activation leads to increased production of reactive oxygen species (ROS) (23,24). To establish a mechanistic understanding for the effects of AC1903 on the Rac1-TRPC5 pathway in podocytes, we measured ROS levels in vitro in podocytes treated with AngII (Fig. 2D). AngII treatment induced a significant increase in ROS, which was blocked by AC1903 and the ROS scavenger *N*-acetylcysteine (NAC) (Fig. 2D). Next, we engineered podocytes to overexpress a well-characterized, constitutively active mutant of the human AT1R, which is unable to inactivate and undergo endocytosis (caAT1R) (25). Increased ROS production was detected in the presence of caAT1R (Fig. 2E). AC1903, ML204, and the Rac1 inhibitor (NSC23677) blocked caAT1R-induced ROS generation (Fig. 2E). We also noted increased podocyte cell death within 36 hours of caAT1R expression (Fig. 2F). By contrast, podocytes treated with AC1903, ML204, or the Rac1 inhibitor were protected from cell death (Fig. 2F). These data suggest that excess ROS production contributes to the molecular events linking Rac1-TRPC5 signaling to podocyte loss.

After characterizing the pharmacokinetic properties of AC1903 (fig. S6), we investigated whether AC1903 could suppress proteinuria in AT1R Tg rats with established disease. Twice-daily intraperitoneal injections of AC1903 (50 mg/kg) for 7 days suppressed severe proteinuria in AT1R Tg rats (Advanced) (Fig. 3A), without evidence of toxicity (fig. S7, A to C). Inside-out electrophysiology measurements in isolated glomeruli from AT1R Tg rats confirmed that AC1903 blocks TRPC5 channel activity during proteinuric disease progression (Fig. 3, B and C). Morphometric analysis demonstrated that treatment with AC1903 led to a significant reduction in pseudocyst formation and in podocyte loss in AT1R Tg rats with advanced disease (Fig. 3, D to F). Thus, AC1903 inhibits the progression of proteinuric kidney disease by preserving podocytes.

To characterize the transcriptional responses to AC1903-mediated inhibition of Rac1-TRPC5 signaling and enhanced podocyte survival in vivo, we compared gene expression profiles [RNA sequencing (RNA-seq)] in isolated glomeruli from WT rats, AC1903-treated AT1R Tg rats in the advanced cohort, and vehicle-treated, age-matched AT1R Tg controls (fig. S8A). We identified 541 differentially expressed genes in AT1R Tg rats compared to WT controls (table S2 and fig. S8B). In support of the hypothesis that Rac1-mediated ROS generation and TRPC5 Ca^{2+} (cation) –mediated signaling lead to disease progression, Gene Ontology (GO) term enrichment analysis revealed ROS-related and cation channel and transporter activity gene signatures (fig. S8C). In line with this, ROS-related genes previously implicated in podocyte injury such as Nox4 (26,27) were found to be up-regulated. After treatment with AC1903,42 genes were differentially expressed in AC1903-treated versus vehicle-treated AT1R Tg rats (table S2 and fig. S8B). This smaller number of genes suggests that AC1903 targets a specific signaling network to confer its therapeutic benefit. GO term enrichment analysis revealed cell adhesion and integrin signaling gene sets,

in support of the notion that AC1903 fortifies the cytoskeleton, prevents pseudocysts, and promotes cell adhesion to prevent podocyte loss (table S2 and fig. S8D).

We also investigated the efficacy of AC1903 in Dahl salt-sensitive (Dahl S) rats, a model of hypertension-induced FSGS (28,29) that recapitulates many of the systemic conditions leading to progressive proteinuric kidney disease in patients. On a low-salt diet, Dahl S rats exhibit progressive, age-related kidney injury with moderate hypertension. On a high-salt diet, Dahl S rats demonstrate progressive nephrotic range proteinuria and decline in kidney function with AngII-mediated hypertension (30,31). We administered AC1903 or a vehicle control to hypertensive Dahl S rats with salt loading (2% NaCl). First, we initiated injection of AC1903 (50 mg/kg twice daily i.p.) into 6-week-old Dahl S rats at the start of 2% NaCl diet (Onset, Fig. 4A). As expected, control rats developed severe and escalating proteinuria within a week of salt administration. By contrast, the rate of progressive proteinuria in AC1903-treated animals was significantly reduced (Fig. 4A). Next, we asked whether AC1903 could suppress progressive proteinuria in rats with more advanced disease. Here, 6-week-old Dahl S rats received 2% NaCl for 1 week, leading to severe, progressive proteinuric disease (Advanced, Fig. 4B). AC1903 treatment was initiated on day 7, and animals were treated for 1 week until day 14 (2-week salt loading). Whereas progressive proteinuria continued to escalate in control rats, AC1903-treated rats had significant suppression of proteinuria (Fig. 4B) with preserved podocyte numbers (Fig. 4C). Morphometric analysis showed that the numbers of podocytes in AC1903-treated Dahl S rats was higher compared to vehicle-treated controls, and similar to the numbers of podocytes in WT and AC1903-treated AT1R Tg rats (~120 podocytes per glomerulus; Figs. 1E, 3F, and 4C). AC1903 had no effect on body weight, blood urea nitrogen, or creatinine in Dahl S rats in these experiments (fig. S9, A to C). Notably, treatment with AC1903 did not affect the mean arterial pressure (MAP), suggesting that the therapeutic benefit is not related to changes in blood pressure but more likely is due to a protective effect on podocytes (Fig. 4D).

Our animal data demonstrate that a specific TRPC5 small-molecule inhibitor administered at the time of severe, established proteinuria, but before creatinine is elevated, can rescue podocytes and attenuate the progression of morphologic and molecular changes that characterize FSGS (fig. S10). These findings provide a mechanistic rationale for therapeutically targeting TRPC5 channels, in contrast to earlier work, which had extrapolated from TRPC6 gain-of-function mutations to suggest a role for TRPC6 inhibition in acquired FSGS (32). Our real-time measurements of single-channel activity in isolated glomeruli show that increased TRPC5 activity is associated with proteinuric disease progression, whereas TRPC6 activity appears to be homeostatic. This is supported by the observation that (in addition to gain-of-function mutations) loss-of-function mutations in TRPC6 also lead to FSGS (33). Our early data with the hypertensive Dahl S rat model support a broader applicability of TRPC5 inhibition as a therapeutic strategy.

In the context of precision medicine, genomic sequencing efforts may help identify a patient population with mutations in genes that result in Rac1 activation for initial clinical studies. Although careful toxicology studies will be needed before taking TRPC5 inhibitors into the clinic, several lines of evidence are reassuring: Rats treated with TRPC5 inhibitor for up to

14 days show no detectable toxicity, and mice genetically lacking TRPC5 from birth show no gross abnormalities, except for an attenuated fear response due to a developmental defect in the amygdala (34). The promising preclinical results with TRPC5 inhibitors suggest that these drugs may form the basis of much-needed, mechanistically based therapies for progressive chronic kidney diseases.

Supplementary Material

Refer to Web version on PubMed Central for supplementary material.

Acknowledgments

We thank T. Tickle for guidance on RNA-seq analysis; K. Maeda for technical assistance with the Dahl S rat studies; L. Gaffney for assistance with graphics; and A. Blobaum and X. Zhan for technical assistance with in vivo pharmacokinetics work. This work was funded by NIH grants DK095045, DK099465, DK103658, DK083511, and DK093746 (A.G.); NIH grant U54-MD007598 (J.M.B.); NIH grant DK103658 (C.R.H.); an F31CA195701 fellowship (A.R.C.); a National Defense Science and Engineering Graduate fellowship (E.-H.S.); a Deutsche Forschungs Gesellschaft fellowship WI 4612/1-1 (N.W.); a Broad–Israel Science Foundation Fellowship (M.D.-L.); and a Deutsche Forschungs Gesellshaft Collaborative Research Center 1118 grant (S.C.H.). A.G. has a financial interest in Goldfinch Biopharma, a biotechnology company focused on discovery and development of precision therapies for patients with kidney disease. A.G.'s financial interest in Goldfinch Bio was reviewed and is managed by Brigham and Women's Hospital–Partners HealthCare and the Broad Institute of MIT and Harvard in accordance with their conflict-of-interest policies. E.S.L. is on the Scientific Advisory Board of Third Rock Ventures (TRV), which is a lead investor in Goldfinch Bio. Under his agreement with TRV, his compensation consists solely of stock in TRV-founded companies. This agreement excludes his receiving stock from certain companies, including Goldfinch Bio. Partners HealthCare–Brigham and Women's Hospital, the University of Nebraska Medical Center, and the authors (A.G. and C.R.H.) have filed a patent application (no. 62/555,219) covering AC1903. The TRPC5 inhibitor compound AC1903 is available from C.R.H. (the University of Nebraska Medical Center) under a materials transfer agreement. All RNA-seq data files are deposited at GEO (accession no. GSE103020).

REFERENCES AND NOTES

1. Jha V, et al. Lancet. 2013; 382:260–272. [PubMed: 23727169]
2. Inrig JK, et al. Am J Kidney Dis. 2014; 63:771–780. [PubMed: 24315119]
3. D'Agati VD, Kaskel FJ, Falk RJ. N Engl J Med. 2011; 365:2398–2411. [PubMed: 22187987]
4. Greka A, Mundel P. Annu Rev Physiol. 2012; 74:299–323. [PubMed: 22054238]
5. Brown EJ, Pollak MR, Barua M. Kidney Int. 2014; 85:1030–1038. [PubMed: 24599252]
6. Akilesh S, et al. J Clin Invest. 2011; 121:4127–4137. [PubMed: 21911940]
7. Gee HY, et al. J Clin Invest. 2013; 123:3243–3253. [PubMed: 23867502]
8. Yu H, et al. J Clin Invest. 2016; 126:1603.
9. Bezzerides VJ, Ramsey IS, Kotecha S, Greka A, Clapham DE. Nat Cell Biol. 2004; 6:709–720. [PubMed: 15258588]
10. Tian D, et al. Sci Signal. 2010; 3:ra77. [PubMed: 20978238]
11. Schaldecker T, et al. J Clin Invest. 2013; 123:5298–5309. [PubMed: 24231357]
12. Wieder N, Greka A. Pediatr Nephrol. 2016; 31:1047–1054. [PubMed: 26490951]
13. Hoffmann S, Podlich D, Hähnel B, Kriz W, Gretz N. J Am Soc Nephrol. 2004; 15:1475–1487. [PubMed: 15153558]
14. Hsu HH, et al. J Mol Med (Berl). 2008; 86:1379–1394. [PubMed: 18773185]
15. Richter JM, Schaefer M, Hill K. Br J Pharmacol. 2014; 171:158–170. [PubMed: 24117252]
16. Miller M, et al. J Biol Chem. 2011; 286:33436–33446. [PubMed: 21795696]
17. Hofmann T, et al. Nature. 1999; 397:259–263. [PubMed: 9930701]
18. Steffes MW, Schmidt D, McCrery R, Basgen JM. Kidney Int. 2001; 59:2104–2113. [PubMed: 11380812]
19. Weins A, et al. Am J Pathol. 2015; 185:2143–2157. [PubMed: 26073036]

20. Kriz W, Lemley KV. J Am Soc Nephrol. 2015; 26:258–269. [PubMed: 25060060]
21. Freichel M, et al. Nat Cell Biol. 2001; 3:121–127. [PubMed: 11175743]
22. Richter JM, Schaefer M, Hill K. Mol Pharmacol. 2014; 86:514–521. [PubMed: 25140002]
23. Buvall L, et al. J Am Soc Nephrol. 2017; 28:837–851. [PubMed: 27628902]
24. Wu RF, et al. J Cell Biol. 2005; 171:893–904. [PubMed: 16330715]
25. Pierce KL, Premont RT, Lefkowitz RJ. Nat Rev Mol Cell Biol. 2002; 3:639–650. [PubMed: 12209124]
26. Sharma K, et al. J Clin Invest. 2008; 118:1645–1656. [PubMed: 18431508]
27. You YH, Quach T, Saito R, Pham J, Sharma K. J Am Soc Nephrol. 2016; 27:466–481. [PubMed: 26203118]
28. Rapp JP. Hypertension. 1982; 4:753–763. [PubMed: 6754600]
29. Zicha J, et al. Physiol Res. 2012; 61(Suppl. 1):S35–S87. [PubMed: 22827876]
30. Garrett MR, Dene H, Rapp JP. J Am Soc Nephrol. 2003; 14:1175–1187. [PubMed: 12707388]
31. Yamada Y, et al. Hypertens Res. 2011; 34:809–816. [PubMed: 21471973]
32. Eckel J, et al. J Am Soc Nephrol. 2011; 22:526–535. [PubMed: 21258036]
33. Riehle M, et al. J Am Soc Nephrol. 2016; 27:2771–2783. [PubMed: 26892346]
34. Riccio A, et al. Cell. 2009; 137:761–772. [PubMed: 19450521]

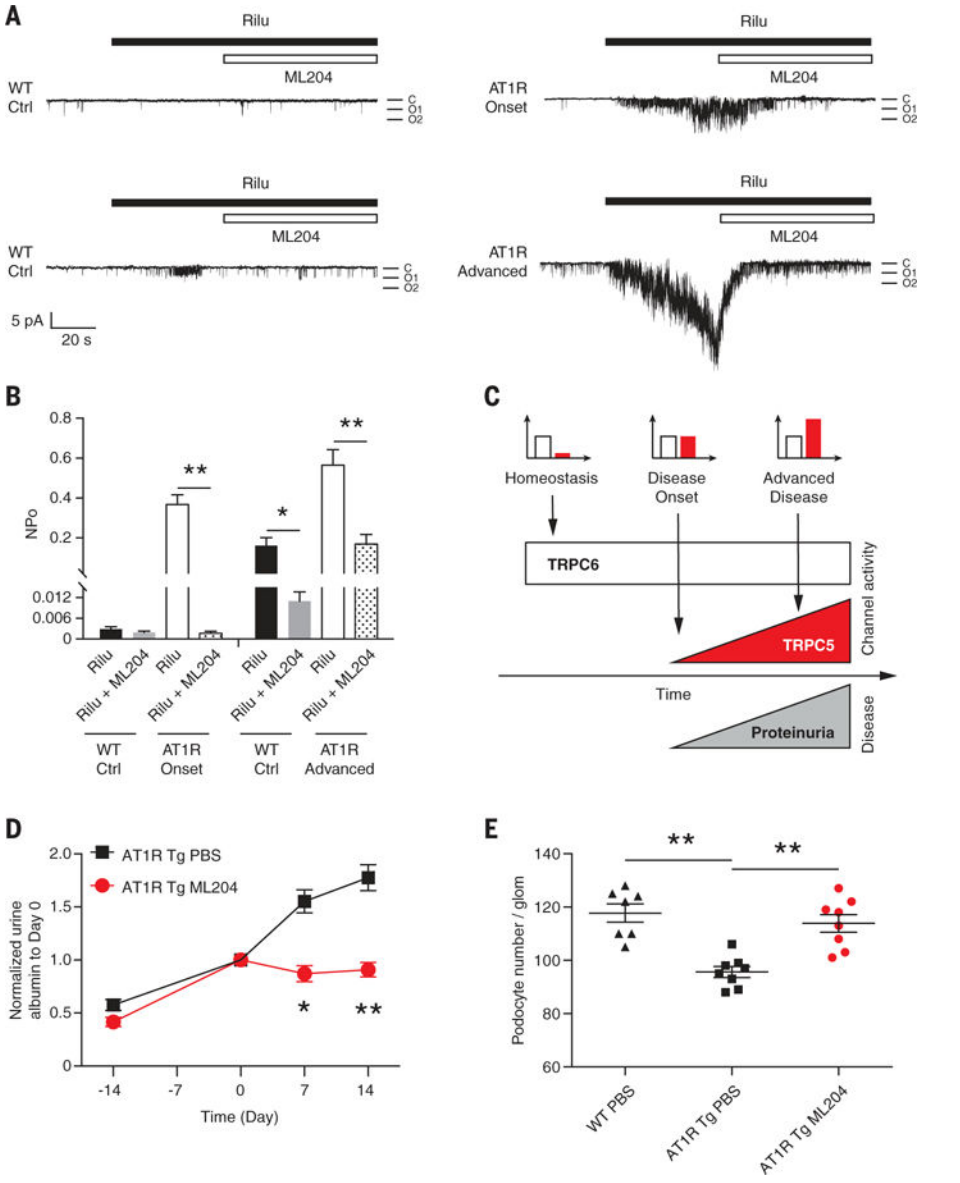

Fig. 1. Escalating TRPC5 ion channel activity correlates with disease progression, and TRPC5 inhibition rescues podocytes in AT1R Tg rats

(**A**) ML204 (1 μM) blocks TRPC5 single-channel activity induced by Riluzole (Rilu, 3 μM) in inside-out recordings from rat glomeruli isolated during early disease (Onset), as compared to barely detectable current in age-matched WT glomeruli (Onset). ML204 blocks a significantly greater Rilu-activated conductance in glomeruli from rats with established disease (Advanced), compared to minimal TRPC5 activity in age-matched WT glomeruli (Advanced). C, close state; O_1, open channel level 1; O_2, open channel level 2. $V_m = -60$ mV. (**B**) Quantification of open channel probability (NPo) for the conductances recorded in (A). WT Rilu $n = 4$ and 5, WT Rilu + ML204 $n = 4$ and 5, AT1R Tg Rilu $n = 4$ and 5, AT1R Tg Rilu + ML204 $n = 4$ and 5 for Onset and Advanced groups, respectively. Mean ± SEM, $^*P < 0.05$, $^{**}P < 0.01$. (**C**) TRPC6 channel activity contributes to podocyte Ca^{2+} homeostasis. TRPC5 activity is coincident with onset of proteinuria and correlates with

FSGS disease progression. (**D**) Progressive proteinuria suppressed by twice-per-day i.p. administration of ML204 in the Advanced cohort of AT1R Tg rats treated for 14 days. AT1R Tg PBS $n = 23$, AT1R Tg ML204 $n = 23$. Mean ± SEM, $*P < 0.05$, $**P < 0.01$. (**E**) Rescue of podocyte numbers in vivo in ML204-treated AT1R Tg rats with established disease (Advanced). WT PBS $n = 7$, AT1R Tg PBS $n = 8$, AT1R Tg ML204 $n = 8$. Mean ± SEM, $**P < 0.01$.

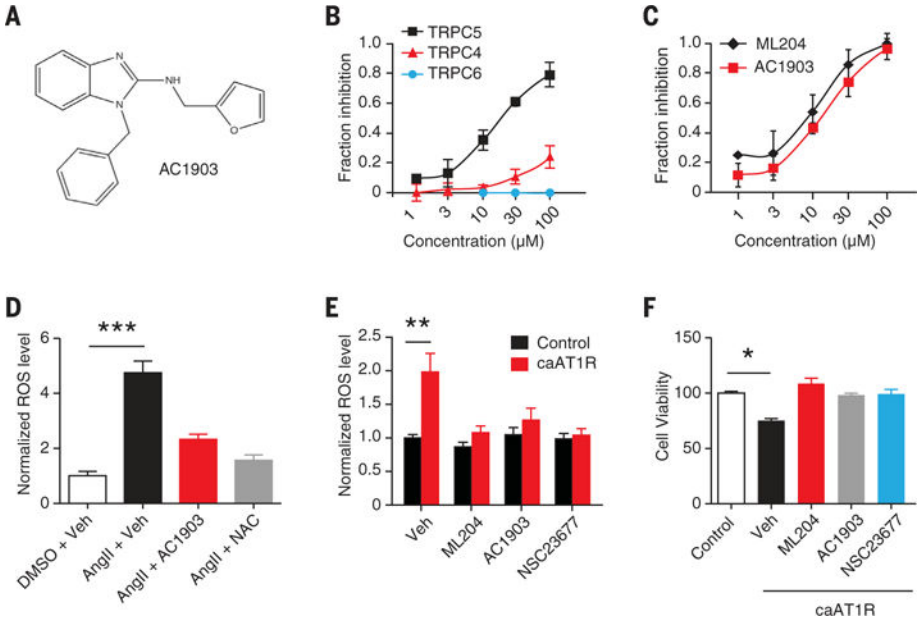

Fig. 2. AC1903, a specificTRPC5 small-molecule inhibitor, protects podocytes from ROS-mediated injury

(**A**) Chemical structure of AC1903. (**B**) Selectivity of AC1903 (1 to 100 μM) for TRPC5 over TRPC4 and TRPC6 in dose-response patch-clamp experiments in the whole-cell configuration. $n > 3$ for each dose. Mean ± SEM. (**C**) Equipotency between AC1903 and ML204 in dose-response patch-clamp experiments in the whole-cell configuration in response to Rilu (3 μM). ML204 $n > 3$, AC1903 $n > 3$ for each dose Mean ± SEM. (**D**) ROS generation blocked by AC1903 (30 μM) in vitro in WT podocytes treated with AngII (10 μM). DMSO, dimethyl sulfoxide; Veh, vehicle. DMSO + Veh $n = 23$, Ang II + Veh $n = 23$, Ang II + AC1903 $n = 24$, Ang II + NAC $n = 24$, each from three independent replicates. Mean ± SEM, $^{***}P < 0.001$. (**E**) ROS generation blocked by AC1903 (30 μM), ML204 (30 μM), and NSC23677 (50 μM) in vitro in caAT1R-expressing podocytes. Veh $n = 40$ and 60; ML204 $n = 40$ and 60; AC1903 $n = 40$ and 60; NSC23677 $n = 40$ and 60, for control and caAT1R-expressing podocytes, respectively, each from four independent replicates. Mean ± SEM, $^{**}P < 0.01$. (**F**) Podocyte cell death rescued by AC1903 (30 μM), ML204 (30 μM), and NSC23677 (50 μM). Control $n = 24$, Veh $n = 24$, ML204 $n = 24$, AC1903 $n = 24$, NSC23677 $n = 12$, each from four independent replicates. Mean ± SEM, $^{*}P < 0.05$.

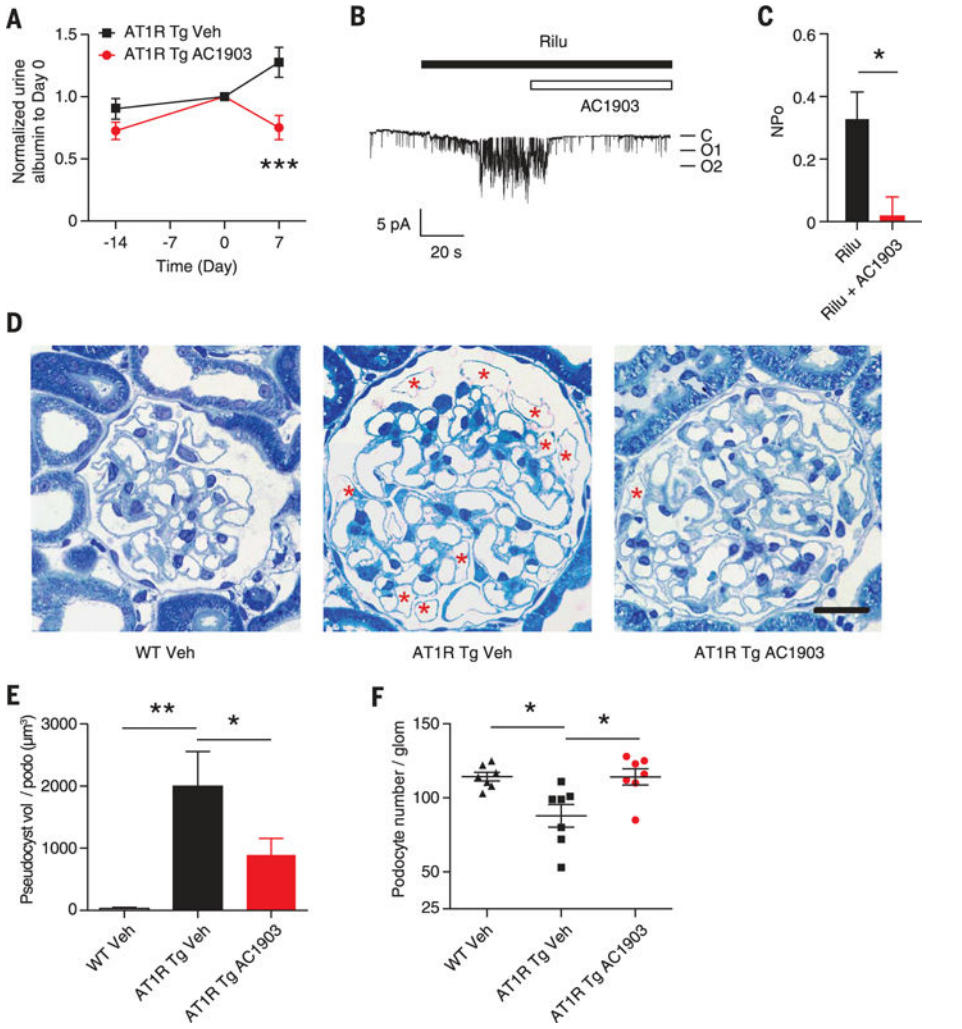

Fig. 3. AC1903 suppresses proteinuric kidney disease progression and rescues podocytes in AT1R Tg rats with advanced disease

(**A**) AC1903 (50 mg/kg) ameliorates proteinuria in AT1R Tg rats with established, advanced disease. Veh $n = 13$, AC1903 $n = 14$. Mean ± SEM, ***$P < 0.001$. (**B**) AC1903 inhibition of TRPC5 channel activity in insideout recordings from advanced-disease AT1R rat glomeruli. (**C**) Quantification of open channel probability (NPo) for the conductances recorded in (B). Each $n = 6$. Mean ± SEM, *$P < 0.05$. (**D**) Toluidine blue semithin sections of rat kidneys. Red asterisks indicate pseudocysts. Bar, 50 μM. (**E**) Reduction of pseudocyst volume in AT1R Tg AC1903 rats compared to AT1R Tg vehicle rats. WT Veh $n = 7$, AT1R Tg Veh $n = 7$, AT1R Tg AC1903 $n = 7$. Mean ± SEM, *$P < 0.05$, **$P < 0.01$. (**F**) Rescue of podocyte numbers in vivo in AC1903-treated AT1R Tg rats with established disease (Advanced). WT Veh $n = 7$, AT1R Tg Veh $n = 7$, AT1R Tg AC1903 $n = 7$, Advanced. Mean ± SEM, *$P <$ 0.05.

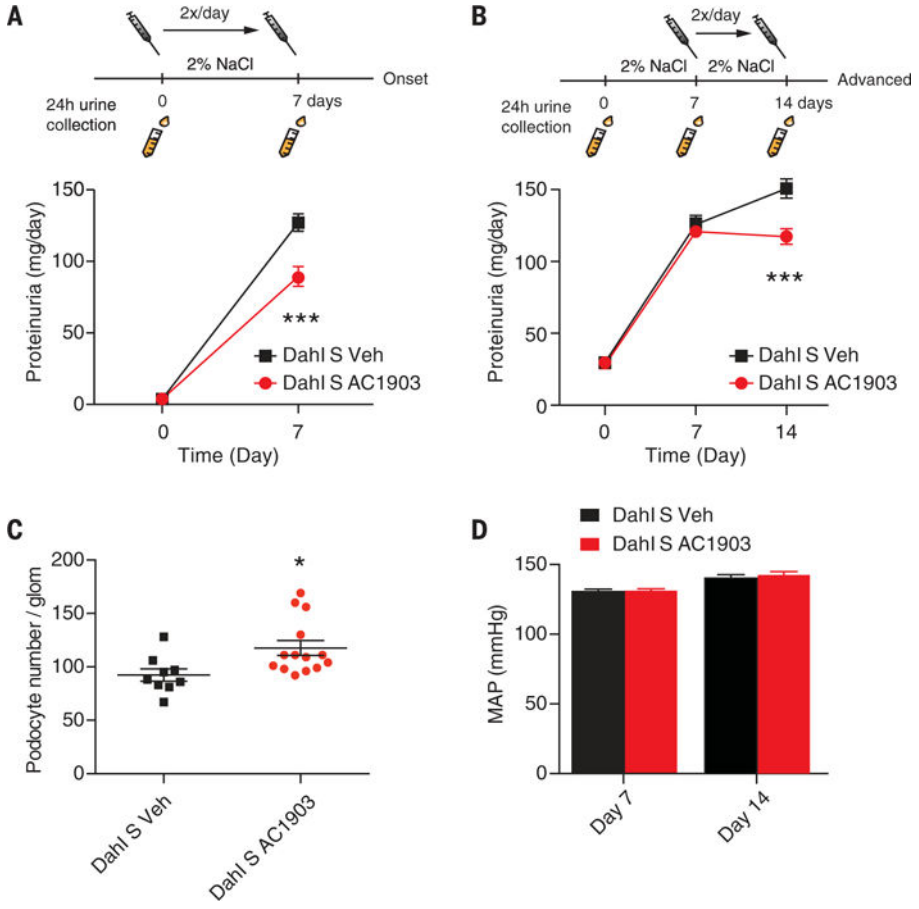

Fig. 4. AC1903 suppresses proteinuric kidney disease progression and rescues podocytes in hypertensive Dahl S rats

(**A**) AC1903 (50 mg/kg) ameliorates proteinuria in Dahl S rats when administered at the same time as high salt intake (Onset). Veh $n = 8$, AC1903 $n = 8$. Mean ± SEM, ***$P <$ 0.001. (**B**) AC1903 (50 mg/kg) suppresses proteinuria in Dahl S rats with established, advanced disease (Advanced). Veh $n = 9$, AC1903 $n = 14$. Mean ± SEM, ***$P < 0.001$. (**C**) Rescue of podocyte numbers in vivo in AC1903-treated Dahl S rats with established disease (Advanced). Veh $n = 9$, AC1903 $n = 14$. Mean ± SEM, *$P < 0.05$. (**D**) Administration of AC1903 has no detectable effect on mean arterial pressure (MAP) of Dahl S rats. Veh $n = 9$, AC1903 $n = 14$. Mean ± SEM.